Chapter 4

Metamaterials in Application to Improve Antenna Parameters

Wojciech Jan Krzysztofik and Thanh Nghia Cao

Additional information is available at the end of the chapter

http://dx.doi.org/10.5772/intechopen.80636

Abstract

In recent years, the demand for miniaturization and integration of many functions of telecommunication equipment is of great interest, especially devices that are widely used in life such as mobile communication systems, smart phones, handheld tablets, GPS receivers, wireless Internet devices, etc. To satisfy this requirement, the mobile device components must be compact and capable of multifunction, multifrequency band operation. An antenna is one of them; it means that it must be conformal to the body of device, reduced in size, and capable to operating at multiple frequencies of mobile communication systems that have been operating on one, so-called smart device. Nowadays, there are many technical solutions applied in the antenna construction to satisfy of those requirements. There are microstrip antenna technology miniaturized by means of high-permittivity dielectric substrate, using shorting wall, shorting pins, some deformation, as the fractal geometry is, and others. However, these methods have disadvantage such as narrow bandwidth and low gain. A new solution that is of great interest to designers is the use of electromagnetic metamaterials for antenna design. The use of metamaterials in antenna design not only dramatically reduces the size of the antenna but can also improve other antenna parameters such as enhancing bandwidth, increasing gain, or generating multiband frequencies of antennas operation.

Keywords: antenna, parameters improvement, bandwidth, gain, multiband, metamaterials, LHM, DNG, ENG, MNG, SRRs, HISs, AMC

1. Introduction

In recent decades, scientists have spent a lot of time and effort in researching new materials and physical phenomena in order to cater to modern life. There are many new artificial materials that have been found to replace the earlier natural materials, which have brought

significant benefits in various areas of life. Metamaterials are among those new materials that are made up of the arrangement of metal structures on the surface of dielectric substrates. Therefore, the physical properties of metamaterials depend on their structures more than the component that makes up them. In fact, materials with negative permittivity and permeability were first studied in 1968 by Veselago, who termed this material such as media left-hand (LH) which is formed by triad's of vectors: electric field, magnetic field, and phase propagation [1]. However, these properties are not available in natural materials but only in artificial materials called metamaterials. The effects created by the metamaterials can be observed during the transmission of electromagnetic waves such as wave propagation. This phenomenon occurs due to an antiparallel group and the phase velocity leads to the inversion of the wave fronts, while its energy is moving away from the source. Metamaterial can be used for microwave and terahertz fields in devices such as antennas, filters, integrated network sensors, or new superlayers that can improve some of the parameters of equipment in the different field of science and technology. The knowledge of metamaterials provides us with a great deal of possibilities for applying and translating the physical concepts of metamaterials from laboratories to innovative antenna designs in practical engineering applications.

A metamaterial is a word derived from the Greek word, it is a combination of the words "meta" and "material," in which "meta" means something beyond normal, altered, changed, or something advance. It is an artificial material designed to obtain the physical properties that do not exist in natural materials. The term of metamaterial was given by Rodger M. Walser, University of Texas at Austin, in 1999 [2, 3]. He defined metamaterials as- "Macroscopic composites having a synthetic, three-dimensional, periodic cellular architecture designed to produce an optimized combination, not available in nature, of two or more responses" [3]. Many definitions are suggested about electromagnetic metamaterials, all of which can give us an understanding of electromagnetic metamaterial as follows:

- Electromagnetic metamaterials (MTMs) are artificial material that is created by arranging homogeneous metal structures and having unusual properties that natural materials are not available.
- The size of an effective homogeneous structure to form a unit cell of metamaterials must be much smaller than the guided wavelength [3].
- Metamaterials are generated by arranging microstructures that are called "atoms" or cells.
- These "atoms" can be made from electrical, nonelectrical, or dielectric materials.
- These structures may be symmetric or asymmetric, isotropic, or anisotropic.
- The arrangement of atoms can be in an orderly or chaotic manner, the purpose of which is to create the desired macrocharacteristics for the metamaterial.

On the other hand, different structures give different types of metamaterials and applications, which are classified based on the material permittivity and permeability values created by those structures [4].

1.1. The properties of metamaterials

The electromagnetic property of these metamaterials can be described by the Maxwell's equations. The transformation of this equation serves to highlight the properties of metamaterials. They are given in the set of equations:

$$\nabla \times \vec{E} = -j\omega\mu \vec{H}; \tag{1}$$

$$\nabla \times \vec{H} = j\omega \varepsilon \vec{E} \tag{2}$$

where $\vec{E}$ and $\vec{H}$ are the vectors of electric and magnetic fields strengths, respectively; ε and μ are the material permittivity and permeability; ω is an angular frequency; and $j = \sqrt{-1}$ is an imaginary number.

In the case of the plane wave propagation, the electric and magnetic fields are represented as:

$$\mathrm{E} = E_0 e^{(-jkr+j\omega t)} \tag{3}$$

$$\mathrm{H} = H_0 e^{(-jkr+j\omega t)} \tag{4}$$

In addition, to evaluate the properties of materials, a general definition of the Poynting power density vector $\vec{S}$ is mentioned, which is subdivided into the time $e^{+j\omega t}$ and the space e^{-jkr} components. The real part of the Poynting vector $\vec{S}$, which determines the energy flow, is represented by the following formula:

$$\vec{S} = \frac{1}{2} \vec{E} \times \vec{H^*} \tag{5}$$

For the plane wave, the electric field $\vec{E}$ and the magnetic field $\vec{H}$ are defined by

$$\vec{k} \times \vec{E} = \omega\mu \vec{H}; \tag{6}$$

$$\vec{k} \times \vec{H} = -\omega\varepsilon \vec{E} \tag{7}$$

In the isotropic and homogeneous medium, the values of ε and μ are simultaneously positive. In this medium, the electric field $\vec{E}$, magnetic field $\vec{H}$, and propagation vector $\vec{k}$ form the right circulate triad of orthogonal vectors. Therefore, it is also defined as the right-handed medium (RHM), where the $\vec{S}$, $\vec{k}$ have the same directions and electromagnetic waves can propagate in them [5].

In that case, the values of ε and μ are negative simultaneously; so, Eqs. (6) and (7) can be rewritten as:

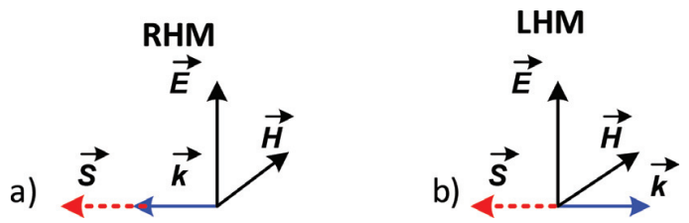

Figure 1. The vectors E, H, k form the trio for right-handed (a) and left-handed media (b).

$$\vec{k} \times \vec{E} = -\omega|\mu|\,\vec{H}\,; \tag{8}$$

$$\vec{k} \times \vec{H} = \omega|\varepsilon|\,\vec{E}\,; \tag{9}$$

In this case, the electric field $\vec{E}$, the magnetic field $\vec{H}$, and the propagation vector $\vec{k}$ form left-hand circulate triad of orthogonal vectors, which also is defined as the left-hand medium (LHM). In this medium, the Poynting vector $\vec{S}$ has the opposite direction to the propagation vector $\vec{k}$, so that it can support backward waves, i.e., the energy and wave fronts travel in opposite directions. **Figure 1** depicts triplet models for RHM (a) and LHM (b) materials.

1.2. Metamaterials classification based on their properties

The metamaterial classification was first proposed by Veselago scientists by considering the permittivity, ε, and the permeability, μ of a homogeneous material. As a result, when ε and μ are simultaneously negative, some abnormal physical phenomena occur such as the reversal of the Snell Law, the reversal of Cerenkov Effect, the reversal of the Doppler Shift. The relationship between the refractive index and the constituent parameters ε and μ is given by the formula:

$$n = \pm\sqrt{\varepsilon_r \mu_r} \tag{10}$$

where ε_r and μ_r are the relative permittivity and permeability of the material, related to the free space permittivity and permeability by $\varepsilon_0 = \varepsilon/\varepsilon_r = 8.854 \times 10^{-12}$ F/m and $\mu_0 = \mu/\mu_r = 4\pi \times 10^{-7}$ H/m, respectively.

From Eq. (10), sign ± of n can get 1 in the four cases, which depends on the pairs of sign of ε_r and μ_r. The electromagnetic metamaterials are classified based on each case of the pair sign ε and μ, they are shown in **Figure 2**. With each region corresponding to the structure created different metamaterials.

In the quadrant I, both parameters ε and μ are positive, and are called Double Positive (DPS) or right-handed medium (RHM). These materials can be found in nature, such as dielectric materials, in which the electromagnetic waves can propagate. In the quadrant II, the parameters are $\varepsilon < 0$—negative, and $\mu > 0$—positive, and such material is called as epsilon negative (ENG) medium, and is represented by a plasma. In the quadrant III, parameters $\varepsilon < 0$—negative, and $\mu < 0$—negative, this region is called double-negative (DNG) or left-handed medium (LHM), and such material could not be find in nature. The quadrant IV $\varepsilon > 0$—positive,

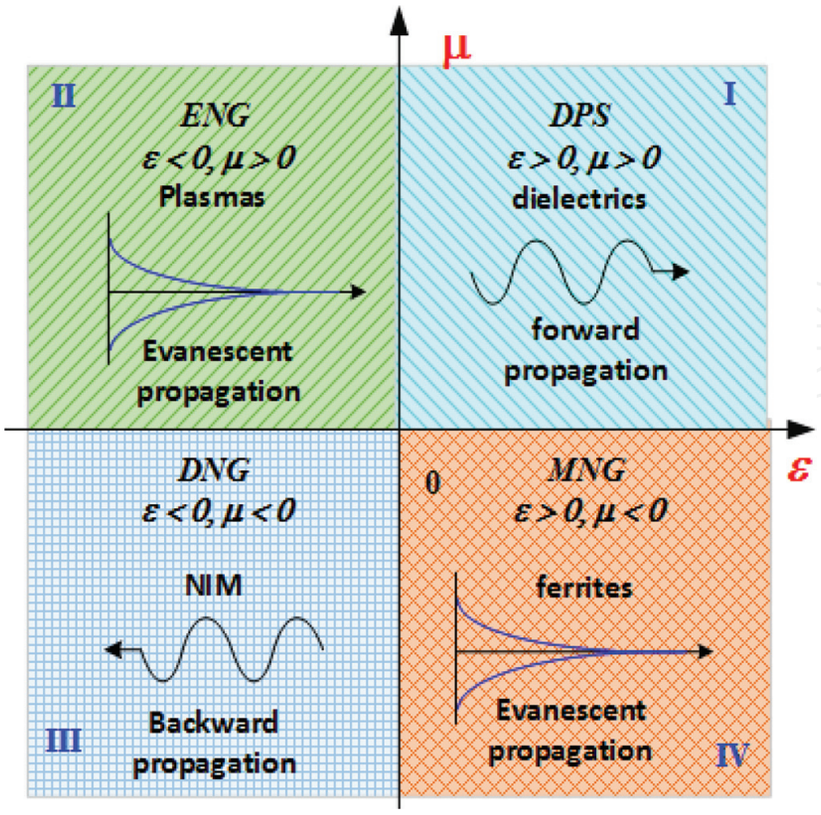

Figure 2. The classification of electromagnetic MTMs based on signs of the ε and μ.

and μ < 0—negative, and such material is called μ—negative (MNG), represented by ferrite materials. Such medium has below plasma frequency. Most waves can propagate in two mediums, namely: at region I and III. Non-propagating evanescent waves are found in regions II and IV [6–9].

Currently, two basic types of structures are being used for designing the most metamaterials: a dense array of thin wires (the electrical dipoles) and an array of split-ring resonators (SRRs) (the magnetic loops).

1.2.1. The epsilon-negative (ENG) metamaterial

The ENG metamaterial uses the metallic mesh of thin wires, for obtaining negative value of ε. These parallel metal wires, which exhibit high-pass behavior for an incoming plane wave, whose electric field is parallel to the wires [10]. The cylindrical array displays the negative permittivity below the plasma frequency, the wire can be made of copper, aluminum, silver, or gold, they are arranged periodically as shown in **Figure 3a**. The effective permittivity is given by the equation [11]:

$$\varepsilon_p = 1 - \frac{\omega_p^2}{\omega^2} \tag{11}$$

where ω is the frequency of the propagating electromagnetic wave and ω_p is the plasma frequency.

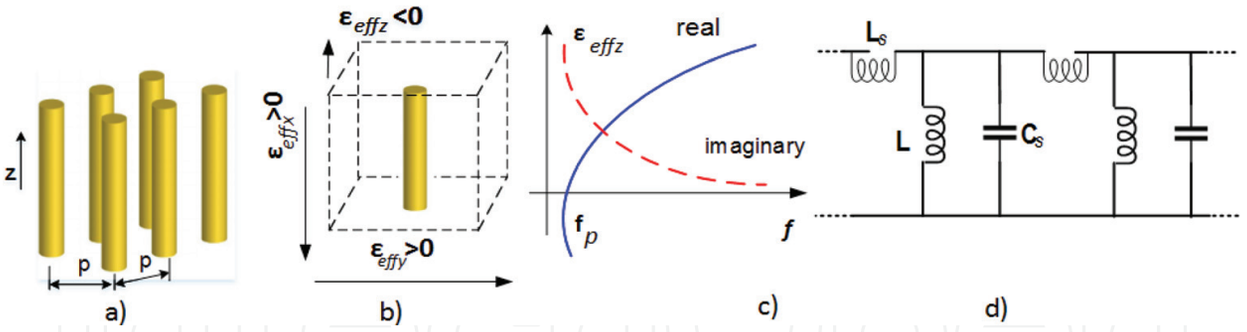

Figure 3. An array of thin conducting wires (a), unit cell (b), plots of the effective permittivity of an array of wires (c), and its equivalent circuit (d).

From Eq. (11), it is shown that when the propagation frequency is below the plasma frequency, its permittivity is negative [12]. This behavior is similar to the propagation of the electromagnetic waves in plasma medium. The propagation frequency as close to the plasma frequency, the value of effective permittivity is increasing. At the plasma frequency, the effective permittivity is equal to zero, and this corresponds to the refractive index equal to zero [13].

Below the cutoff frequency of the array, there is no wave propagation, and the electromagnetic waves are totally reflected waves. This behavior is similar to the propagation of electromagnetic waves in the plasma medium. The plasma frequency depends on the lattice constant p and the radius of the individual wire. If the lattice constant frequency is several times smaller than the wavelength, the wire array can be considered as an equivalent of the continuous plasma [13, 14].

1.2.2. The mu-negative (MNG) metamaterial

As the mu-negative (MNG) material, the most popular structure has been using is split ring resonators (SRRs). A unit cell of the SRR is composed of two concentric metallic rings (can be circle or square) and separated by a gap d (see **Figure 4b**). Each ring has a narrow slot, and they are spaced 180 degree apart on each side. The gap between inner and outer ring acts as a capacitor, while the rings themselves act as an inductors. Therefore, the combination of the two rings acts as an LC resonance circuit. The effective permeability of MNG metamaterials is given by the formula (12):

$$\mu_{eff} = \mu'_{eff} - j\mu'_{eff} = 1 - \frac{f_{mp-}^2 f_0^2}{f^2 - f_0^2 - j\gamma f} \tag{12}$$

where f is the frequency of the signal, f_{mp} denotes the frequency at which (in the lossless case) $\mu_{eff} = 0$ ("magnetic plasma frequency"), f_0 is the frequency at which μ_{eff} diverges (the resonant frequency of the SRR), and γ represents the losses. The frequencies f_{mp} and f_0 depend on the lattice constant (p), and the geometry parameters of the SRR such as inner and outer radii of the rings, the width of the gap between the rings, and the slit width [15]. The dependence of μ_{eff} on the frequency is shown in **Figure 4c**.

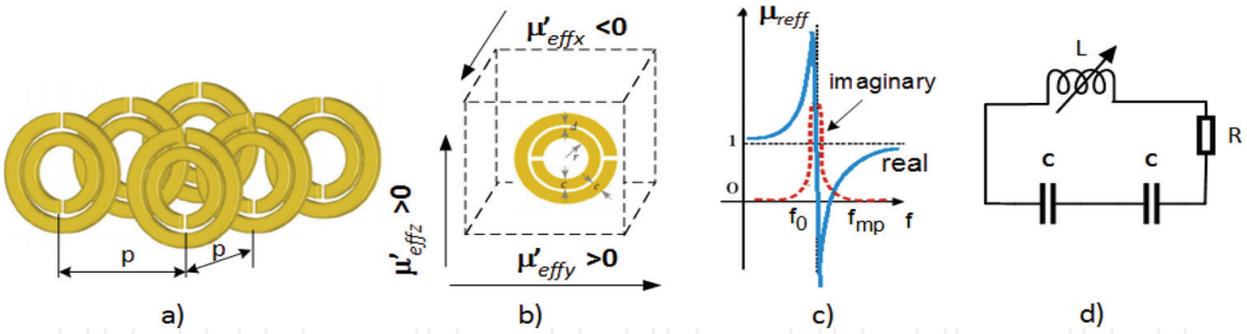

Figure 4. An array of SRRs (a), SRR unit cell (b), the effective permeability of SRR array (c), and equivalent circuit (d).

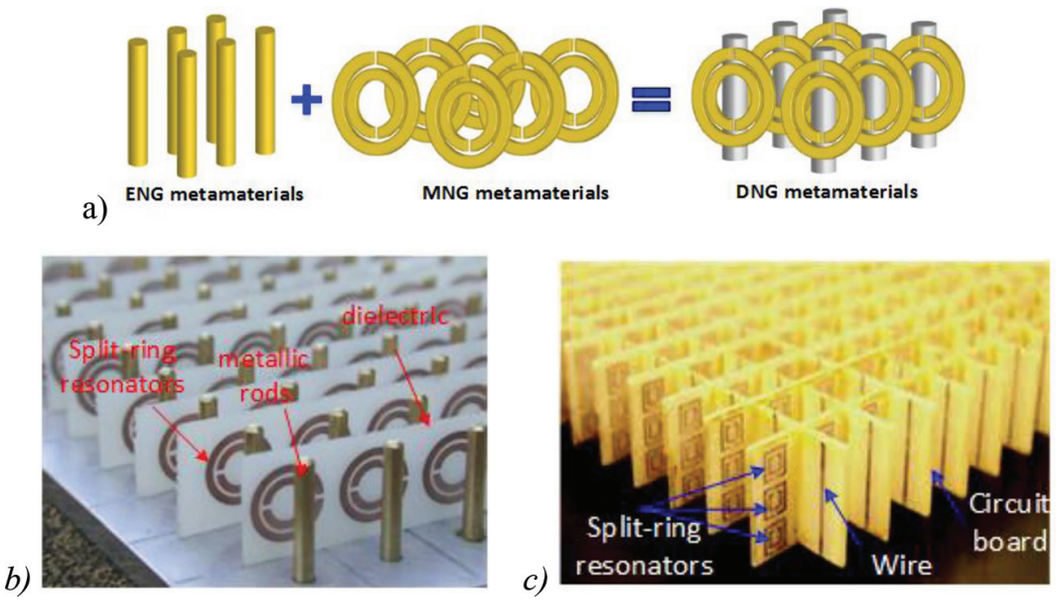

Figure 5. Combination of thin wires and SRR to form DNG metamaterials (a) and examples of realizations of DNG metamaterials (b) and (c).

1.2.3. The double-negative (DNG) metamaterial

The DNG metamaterial is also known as the negative refractive index material (NIM). The properties of the metamaterials DNG were first achieved by combining the thin wire-based ENG structure with SRR-based MNG structure (**Figure 5a**) [16]. This combination satisfies the requirement of $\varepsilon < 0$ from a wire/rodded medium (as an artificial dielectric) and $\mu < 0$ from a split ring resonator (SRR). The first structure was constructed from the combination of planar SRRs etched on a thin dielectric layer and metallic rods (**Figure 5b**). In addition, to take advantage of the two sides of the dielectric layers, two-dimensional metamaterials have been designed by engraving the SRR on one side of the dielectric layer and planar strips on the other [17] (**Figure 5c**).

Because of DNG is made up of thin wire medium and SRRs medium, which their strong resonance behavior (Drude-Lorentz models) affects the frequency. Therefore, the generated DNG metamaterials are also dependent on frequency, which results in the refractive index n being reformatted as:

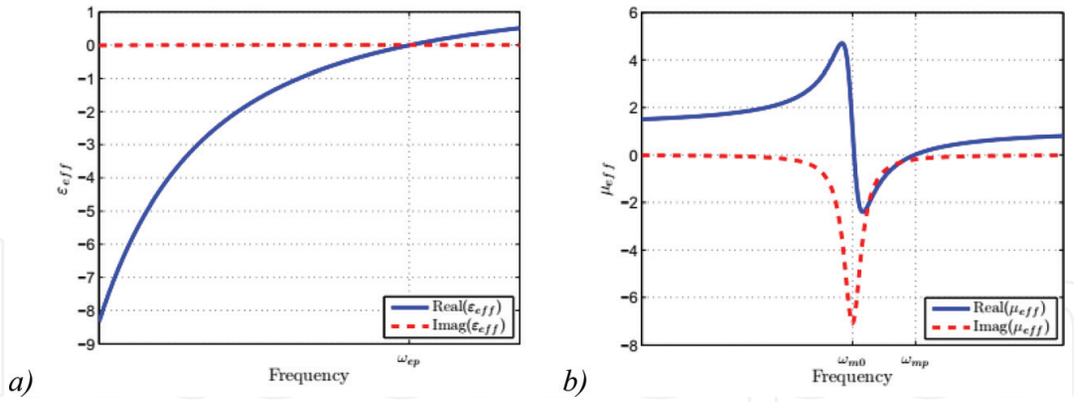

Figure 6. The plots of effective permittivity (a) and permeability (b) of the DNG metamaterial.

$$n \equiv n_{eff}(\omega) = \sqrt{\varepsilon_{eff}(\omega)\mu_{eff}(\omega)} \tag{13}$$

where $\varepsilon_{eff}(\omega)$ and $\mu_{eff}(\omega)$ are the frequency-dependent effective permittivity and the effective permeability, respectively.

These effective material parameters are characterized by their Drude-Lorentz dispersion models and have the form described in Eqs. (14) and (15)

$$\varepsilon_{eff}(\omega) = 1 - \frac{\omega_{ep-}^2 \omega_{e0}^2}{\omega^2 - \omega_{e0}^2 + j\omega\gamma_c} \tag{14}$$

$$\mu_{eff}(\omega) = 1 - \frac{F\omega^2}{\omega^2 - \omega_{m0}^2 + j\omega\Gamma} \tag{15}$$

where ω_{ep} and ω_{mp} are the electric and magnetic plasma frequencies, respectively, ω_{e0} and ω_{m0} are the electric and magnetic resonant frequencies, respectively, γ_c is the collision frequency, F is an amplitude factor, and Γ is a damping factor.

These expressions have been plotted in **Figure 6**.

To get the DNG metamaterial from the combination of the ENG and MNG structures, both negative regions of them must coincide. Then, the ENG domain is found corresponding to $\omega_{e0} < \omega < \omega_{ep}$ and the MNG region corresponding to $\omega_{m0} < \omega < \omega_{mp}$. Note that, if the wires are electrically continuous, their resonant frequency is 0 ($\omega_{e0} \approx 0$). This leads to results, since the ENG region is wider compared to the MNG region, the magnetic resonator metamaterial limits the DNG performance, when assembled together with an electric resonator metamaterial.

2. Metamaterials in antenna design

Due to the special physical properties that natural materials do not exist, nowadays, the metamaterials are very attractive materials and are applied in many areas of life, such as the

microwave invisibility cloaks, the invisible submarines, the revolutionary electronics, the negative refractive-index lenses, the microwave components, as the filters, compact, and efficient antennas [18]. Applying metamaterials to design of antennas is one of its most important applications [19, 20].

Because metamaterials have unusual properties, so we can create antennas with novel characteristics, which cannot be obtained with traditional materials. The metamaterial antenna is one or more layers of metamaterials that are used as substrates or in addition to the configuration of the antenna to improve its performances [21–23]. From scientific research shows that the application of metamaterials in the antenna design can enhance the radiated power, improve some important parameters and reduce the size of the antenna. Depending on the design purpose of the antenna, the choice of structure and method of application of metamaterials varies.

2.1. Unit cell of metamaterials

The metamaterials applied in the antenna design can be in the form of a unit cell or multiple unit cells assembled together into an array. Thus, the first step in designing the antenna metamaterials is to design and analyze the main factors affecting the resonance frequency, permittivity, and permeability of its unit cell [24]. The design of unit cells of metamaterials is based on the calculation of size and simulation of unit cells, so that the parameters ε and μ of these unit cells will satisfy the requirements at the expected resonant frequency. Depending on the structure and size of each unit cell, we can obtain different ε, μ, and resonant frequencies f. For each unit cell type, the dimensions of unit cell can be adjusted to satisfy condition at resonant frequency f_r [25]. A unit cell is usually smaller than 1/10 of the operating wavelength (see **Figure 7**), depending on the shape of the metamaterial, but the unit cell size is different [19, 20, 26].

For example, a unit cell of metamaterial is designed and simulated based on the steps below. The size of the unit cell, in order for the metamaterial to satisfy the homogeneous conditions, the unit cell size must be much smaller than their guided wavelength. The unit cell of metamaterials at 1.88 GHz for GSM cellular phone system is shown in **Figure 8** [27].

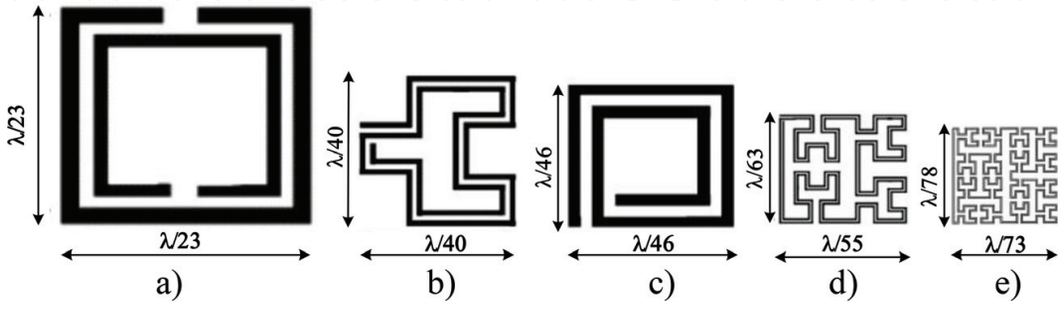

Figure 7. A unit cell of an inclusion with the SRR (a), second-order Hilbert fractal inclusion (b), square spiral (c), third-order Hilbert fractal inclusion (d), and fourth-order Hilbert fractal inclusion (e). Note that as the order of Hilbert fractal curve increases, the size of inclusion decreases.

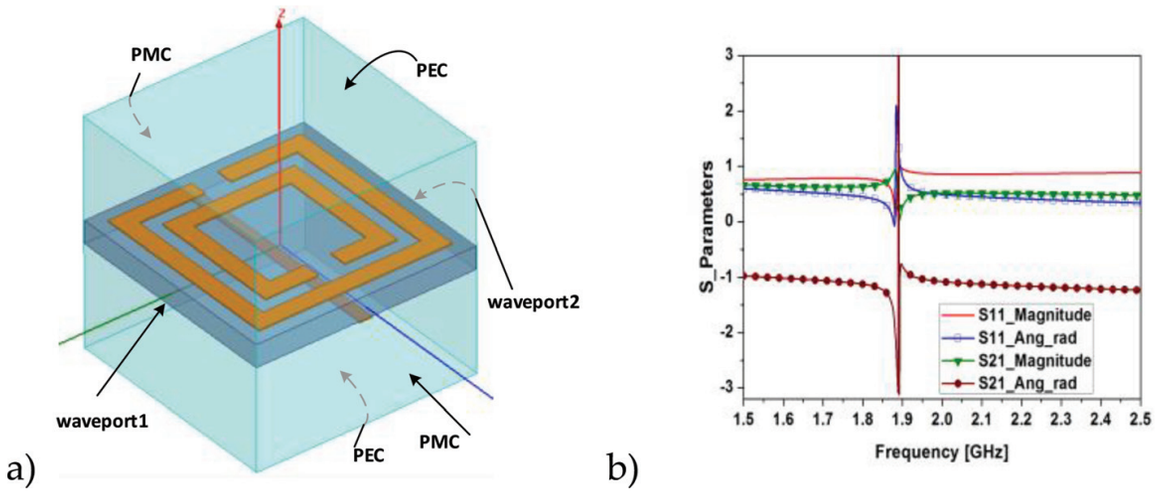

Figure 8. The unit cell of SRR simulation model (a) and the plots of S-parameters (b) at 1.88 GHz for GSM cellular phone system.

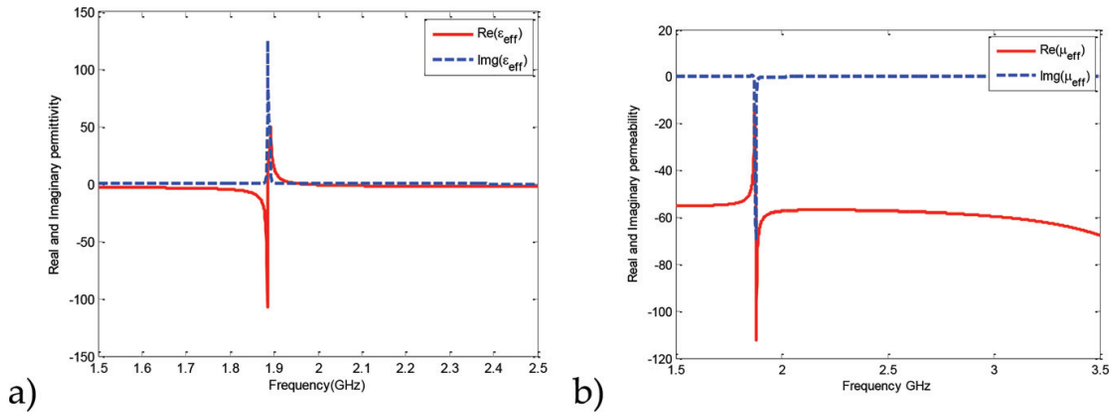

Figure 9. Effective permittivity (a) and permeability (b) of metamaterial retrieved from S-parameters at 1.88 GHz [27].

The model of a SRR unit cell is shown in **Figure 8a**. The perfect electric conductor (PEC) boundary condition is applied to the z-axis, and the y-axis is defined as a perfect magnetic conductor (PMC) for the surfaces of the radiation box [28]. The *S*-parameters of unit cell including S_{11}, S_{21} are exported as magnitude and phase (**Figure 7b**). The parameters ε and μ of the metamaterials must be verified through the *S*-parameters of unit cell given by formulas (16)–(19) and can extract them into graphs by the MATLAB program (**Figure 9**) [29].

$$z = \pm\sqrt{\frac{(1+S_{11})^2 - S_{21}^2}{(1-S_{11})^2 - S_{21}^2}} \tag{16}$$

$$n = \frac{1}{k_{0d}}\left\{\left[Im\left[\ln\left(e^{ink_0d}\right) + 2m\pi\right] - iRe\left[\ln\left(e^{ink_0d}\right)\right]\right\}\right. \tag{17}$$

$$e^{ink_0d} = \frac{S_{21}}{1 - S_{21}\frac{z-1}{z+1}} \tag{18}$$

$$\varepsilon = \frac{n}{z}; \mu = nz \tag{19}$$

where S_{11} and S_{21} are the reflection and transmission coefficients, respectively; k_0 is the wavenumber; d is the maximum length of the unit element; m is the integer related to the refractive index of n; and z is the wave impedance; μ is the permeability; and ε is the permittivity.

In many cases, the numerical simulations of unit cells, according to calculations, do not fully achieve the desired results. Thus, the sizes of the unit cells need to be adjusted iteratively, until the simulation results satisfy the requirements of the metamaterial structure. For simulation results to be satisfied in the shortest possible time, the size of unit cells can be determined using an optimization computational algorithm. In Ansoft HFSS software, we can use the optimization method to save time and get the results as expected. Optimization algorithm of the unit cell size is shown in the diagram in **Figure 10**.

To save the time and load of the processor of the computer, choosing the value of parameters should be optimized in the two stages. In the first stage, we should select the start value, the end value of the parameters which are not too close to the calculated value, and the step value is not too small. After optimization, we select the desired results (if achieved). If the results are not satisfactory, we proceed with the optimization by selecting the optimal parameters, which give the result closest to the desired. Then proceed to select the start value, the value close to the selected value in the previous optimization, the value of the step is smaller than the previous step. The optimal execution will result in the most satisfying results.

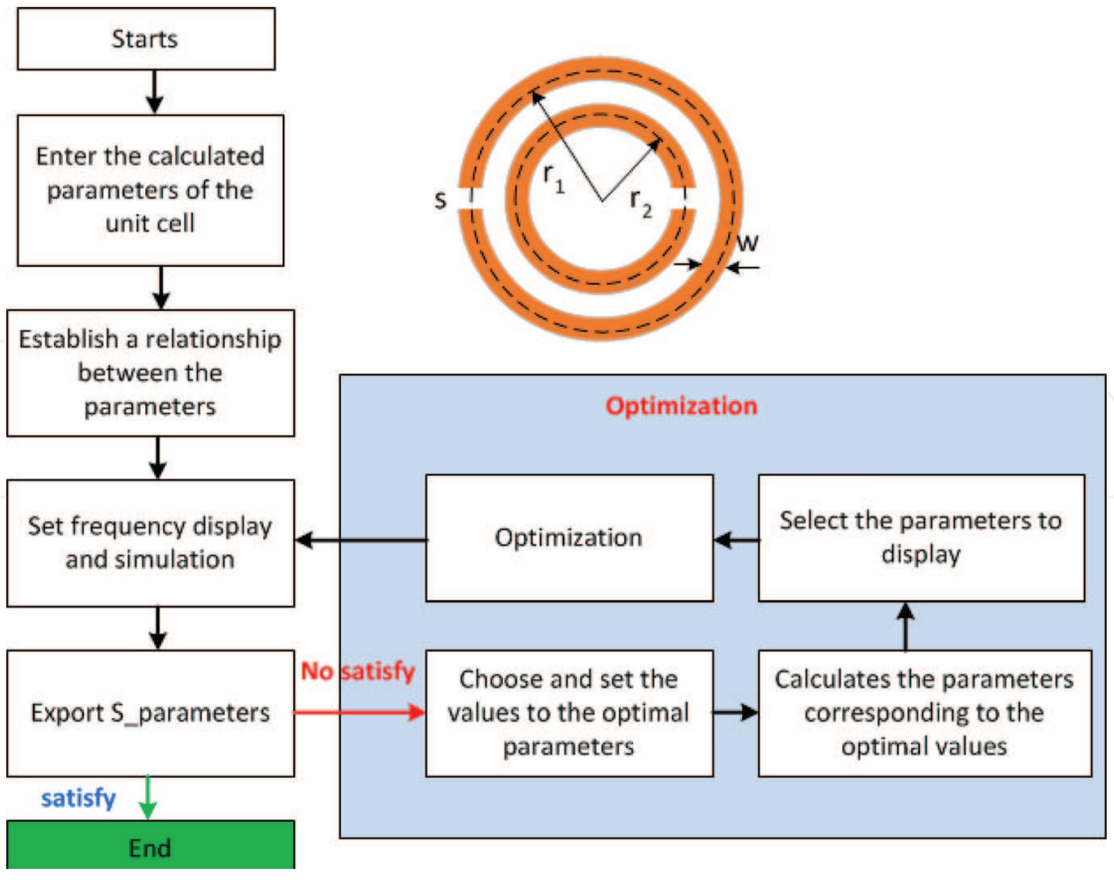

Figure 10. Optimal algorithm in designing unit cells of metamaterial.

2.2. The functions of metamaterials in antenna design

In the antenna applications, among the applications of microwave and radio frequency substrate materials, the artificial magnetic conductors (AMCs) and the high-impedance surfaces (HISs) are the most relevant and applied devices. They are used to design compact and low-profile antenna systems by placing HISs or AMCs around or close to the antenna radiating elements. In addition, metamaterials can also be used as part of the antenna structure or the feeding part of the antenna system.

2.2.1. Metamaterials used as the antenna environment

Metamaterials are applied as the antennas environment, to improve their radiation properties by using the artificial magnetic conductor (AMC). It is a type of implemented metamaterial in several antennas and microwave design applications. By utilizing the unique characteristics of metamaterials which do not exist naturally, the performance of various microwave devices can be enhanced. The property limits the applications of AMC in wideband antenna applications. One of the techniques to improve the narrow band AMC as the ground plane is discussed in detail. The employment of AMC has solved many issues while overcoming the typical limitations in conventional antenna designs. To improve the radiation properties of the antenna by using metamaterials, antennas are often placed above the reflector in order to radiate in one direction only, while reducing the back-radiation [30]. In this case, the metamaterial is not used as a medium but as a device, which serves as active substrate for the creation of plasma environment in each unit cell of the metamaterial. The distance between the antenna and the metal surface should be chosen for a minimum of $\lambda/4$, where the metamaterial acts as a reflective plane to enhance the radiation, it is shown in **Figure 11** [31]. This can be explained by means of image theory for electric or magnetic currents. When placing a charge $\rho\left(\vec{r}\right)$ or current $\vec{J}\left(\vec{r}\right)$ distribution close to a conductor, there are several charges and currents that appear on the surface of the metal, which are involved in the radiation of the conductor. Both perfect magnetic conductors (PMCs) and perfect electric conductor (PECs) boundary conditions (BCs) are appearing these image current [32]. Depending on the type of reflector, the images of the electric or the magnetic current will change. **Figure 11b** and **c** shows the

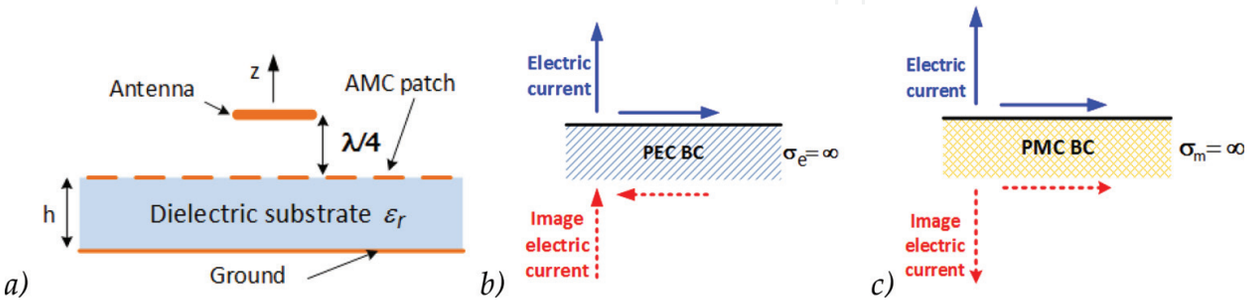

Figure 11. Geometry of an antenna located above an AMC ground plane (a), the electric image currents due to a PEC (b) or a PMC (c) boundary condition (BCs).

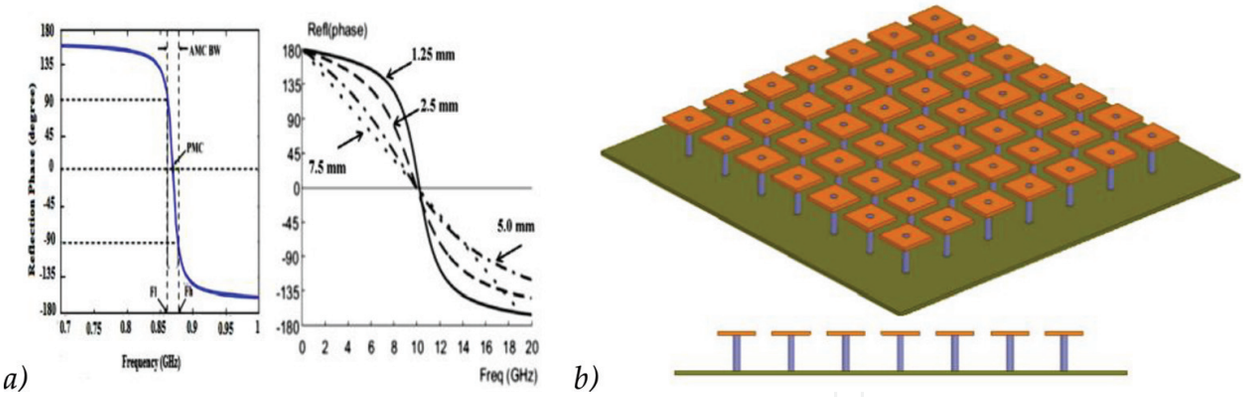

Figure 12. Typical reflection phase diagram of AMC (a) and mushroom-like surface design (b).

electric currents (of a dipole antenna) placed above a PEC and a PMC boundary conditions (BSc).

ACM is a widely used metamaterial in antenna design, it is used to mimic the behavior of PMC, which is not available in nature. The performance of the antenna is improved when it is combined with ACM. Because with this combination, the ACM mimics the PMC is the ability to provide zero-degree reflection phases at its resonant frequency (**Figure 12a**) [33].

One of the first AMC surfaces was the electromagnetic band-gap (EBG) surface, which was introduced by Sievenpiper in 1999 [34]. The so-called mushroom-like surface is composed of a ground plane loaded with a lattice of square patches which are connected to the ground plane through metallic vias, as shown in **Figure 12b**.

Previous ACMs was fabricated using a planar dielectric substrate double-side metallized, where one side is a ground plane, whereas on another side, the square patches are photo-etched. The metallic bars are inserted into the substrate to connect two sides (ground plane and individual patches) of the AMC. In addition, other AMCs are designed that do not require a ground plane for reflective purposes. One layer with capacitive-loaded loops (CLLs) of the volumetric AMC is seen in **Figure 13a**.

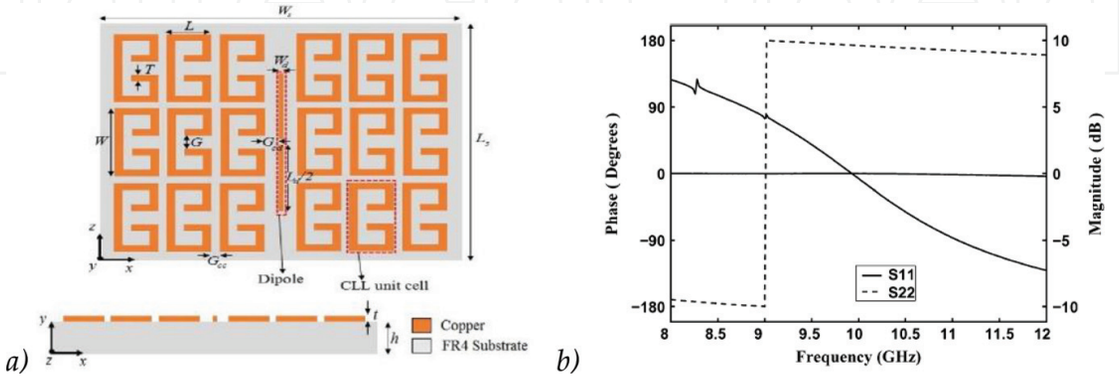

Figure 13. Schematic of proposed two fins CLL loaded dipole antenna (a) and the phase of the reflection coefficients of S_{11} and S_{22} (b).

An electric field plane wave linearly polarized along the y-axis impinges the volumetric CLL metamaterial block along the +x direction (port 1), or along the −x direction (port 2). In such a case, the phase of the reflection coefficient S_{11} in **Figure 13b** shows a PMC response (phase (S_{11}) = 0°) around 10 GHz. It is also interesting to note that the phase of S_{22} remains around the value of ±180° [35].

2.2.2. Metamaterials as part of antenna structure

Metamaterials can be used as part of the antenna structure, which aims to design a compact antenna size without deteriorating performance of its. In this case, the metamaterials are used with high permeability values ($\mu >> 1$) as a magneto-dielectric (MD) substrate of patch antennas [36, 37]. As a result, the size of the antenna is significantly reduced without using a high permittivity ($\varepsilon >> 1$). **Figure 14** shows the patch antennas minimized by the application of MD (a) and comparison with shifting of resonance frequencies for different substrates: air, dielectric, and magneto-dielectric.

In addition, the metamaterials as part of the antenna are also applied in the left-handed transmission line (LH-TL) properties, typically the dipole antenna (**Figure 15a** and **b**).

In this case, the transmission line with left-handed loading actually operates as a composite right-/left-handed transmission line (CRH/LH TL) due to the parasitic effect [38]. **Figure 15c** shows the equivalent circuit model of the lossless unit cell, where the shunt inductors L_L and capacitors C_L act as an LH transmission line, while the shunt capacitors C_R and capacitors L_R act as right-handed (RH) transmission line [39].

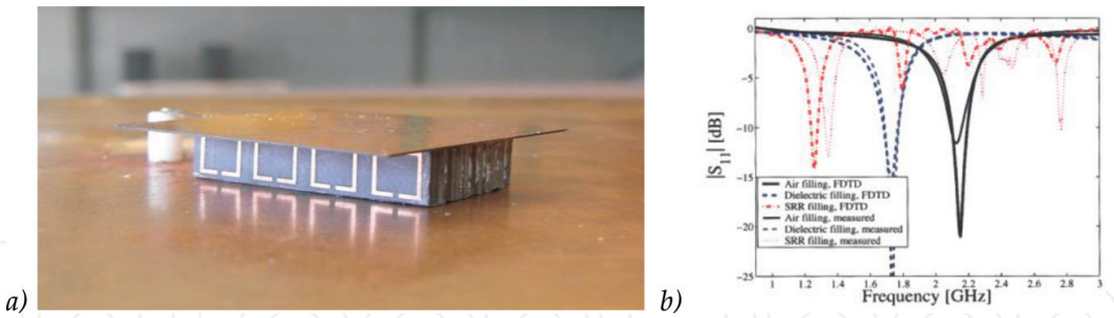

Figure 14. Patch antenna with high-μ metamaterial substrate (a) and input impedance plots for different substrates air, dielectric, and magneto-dielectric (b).

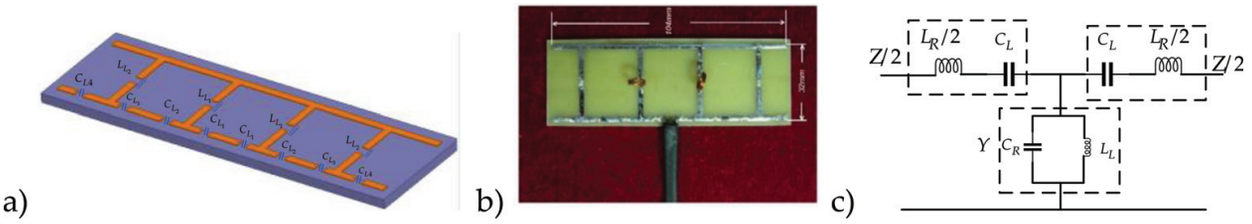

Figure 15. The simulation model (a) fabricated (b) of the left-handed dipole antenna, and the equivalent circuit model of the lossless unit cell of the CRLH dipole (c) [38].

2.3. The effects of applying metamaterials in antenna design

Using metamaterials in antenna design may lead to reduced size, improve gain, enhance bandwidth or to create multiband antenna. Depending on the technical requirements of the designed antenna, the metamaterials will be used as different functions of the antenna.

2.3.1. The metamaterials in improving gain of antennas

Low gain is a main disadvantage of small planar antennas, which must be overcome to satisfy transceiver systems overall energetic ling budget. In addition to using an array antenna, recently the metamaterial is a solution that has been applied in antenna design. In this case, the used metamaterials may be artificial magnetic conductors (AMCs) or artificial magnetic materials (AMMs). They are applied as the environment of the antenna in such a way as to arrange the unit cells of the metamaterials surrounding radiated elements of the antenna [40], or using one or more superstrates above or below the radiated elements [41], or using such as metamaterials as the loading of the antenna [35, 42]. **Figure 16** shows the applied methods of metamaterials for improving gain of antenna.

Each of these methods has different advantages and disadvantages. The ability to improve antenna power gain depends on the number of superstrate, the type of unit cell, and distance between the radiation elements to the superstrates.

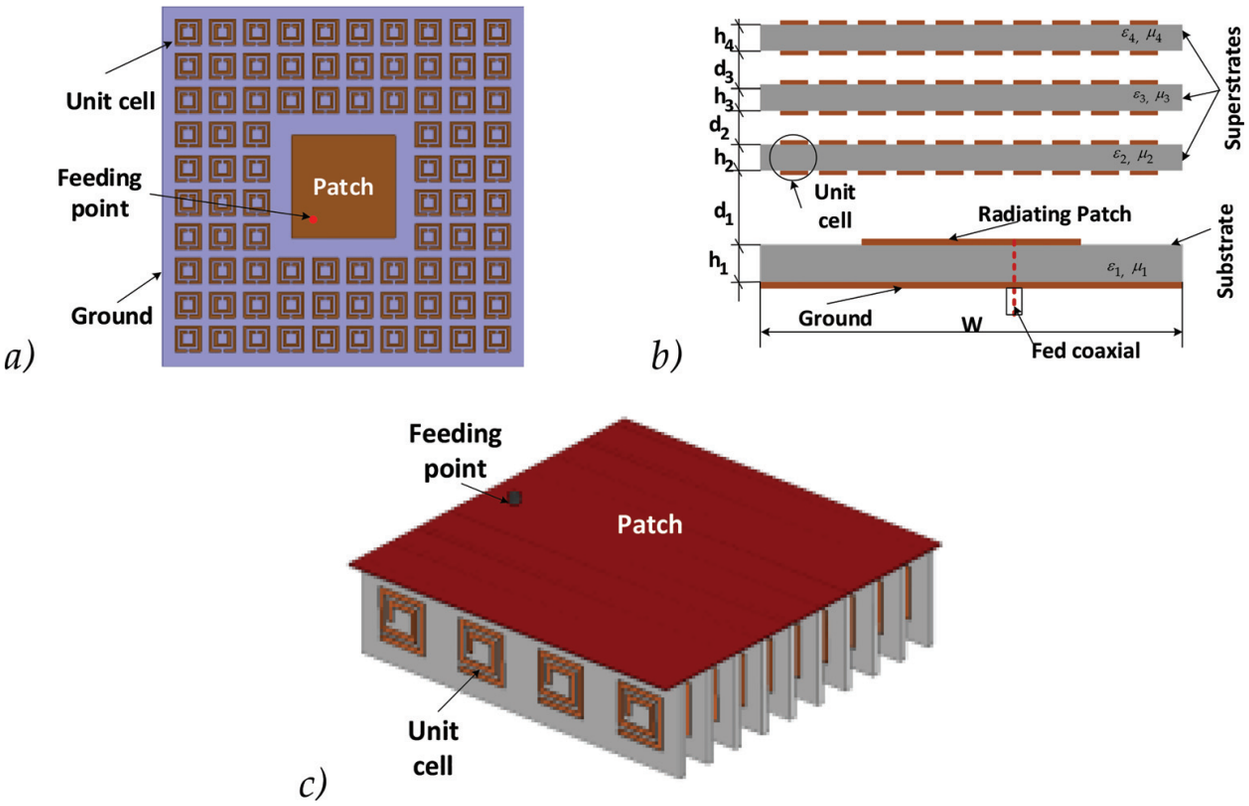

Figure 16. Models of metamaterials application in improving the power gain of the antennas: unit cells surrounding the radiated patch (a), metamaterials as superstrate (b), using the metamaterials as antenna loading (c).

In the case, the unit cells of metamaterials arranged around the radiation elements of the antenna, they can be loaded to one side or both sides of the substrate. The size of these unit cells must be investigated, so that the metamaterials have special physical properties that match the resonant frequency of the antenna. The unit cells are easily integrated with radiated elements and can be used as insulators to reflect surface waves based on negative μ characteristics. By inserting the unit cells of MTM, loaded around the conventional antenna, the antenna radiation efficiency increases, and the power gain is higher than ≥2 dB [39]. Depending on the number of unit cells, as well as resonant frequency of the designed antenna, the achieved gain may be also different.

In the case, when the metamaterials are placed on another dielectric layer called superstrate, the unit cells of metamaterials are loaded on a different dielectric with the distance d from the radiation elements to the superstrate. These array unit cells created AMCs or AMMs, which can be loaded in one side or both sides of the superstrate. The power gain of an antenna depends on the number of superstrate, the number of unit cells, and the distance from the radiation elements to the superstrate [43, 44]. This is shown in **Figure 17**.

The application of metamaterials as a superstrate in antenna design has significantly improved the achieved gain. However, this method also increases the size and thickness of the antenna.

2.3.2. The metamaterials in reducing the size of antennas

There are many technical solutions that have been used to design compact antennas such as high-permittivity dielectric substrate of microstrip antennas, shorting pins, shorting walls, inserting some disturbances into antenna structure, applying the fractal geometry, etc. Recently, many designers have used metamaterials as a defected ground structure (DGS) to reduce the size of the antenna. In this case, the unit cells of the metamaterials have unusual properties at the resonance frequency of the designed antenna; the dimension of these unit cells is equal to the size of the removed parts of the DGS [45]. **Figure 18** shows the simulation models of the two antennas, both of which operate at 1.88 GHz for the GSM system.

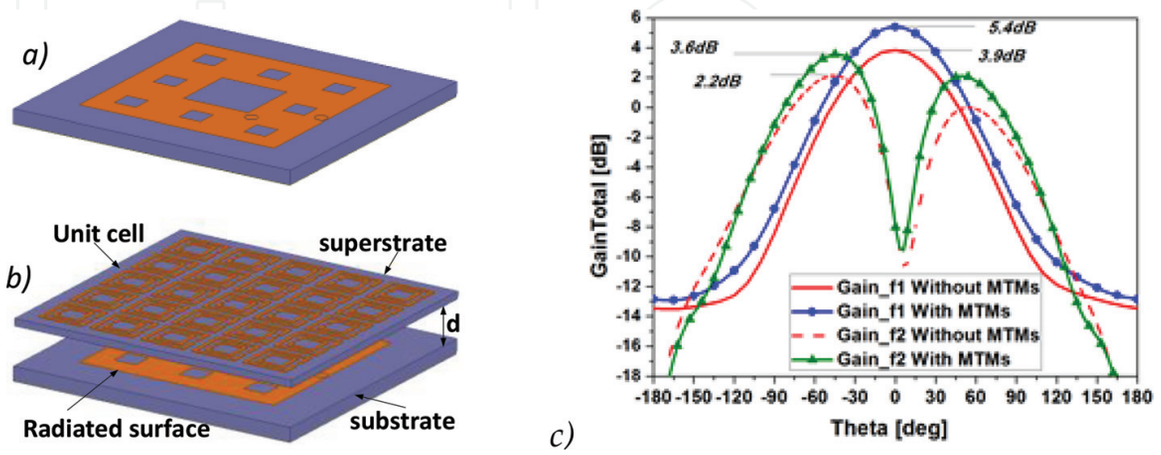

Figure 17. The Sierpinski carpet fractal antenna (a), the antenna (a) covered with the AMC MTM (b), and realized antenna power gain (c), for two resonant frequencies [43, 44].

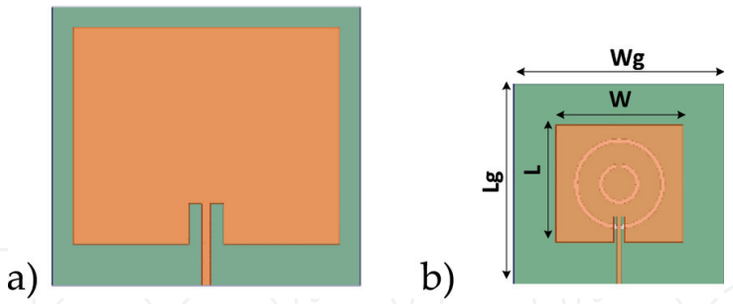

Figure 18. Comparison of the size of microstrip patch antenna MPA without loaded CSRR (a) and with loaded CSRR (b) for GSM system [27].

Types of microstrip patch antennas	Overall antenna size [mm × mm]	Type of radiation patterns	Antenna size ratio, %
Without MTMs	53.28 × 62.08	Directional	100
With MTMs	23.28 × 25.03	Directional	60

Table 1. Comparison between parameters of two types of antennas for GSM cellular phony.

The dimensions of microstrip antenna (**Figure 18a**) are bigger than dimensions of microstrip antenna with complementary split ring resonator (CSRR) designed on the antenna ground plane (**Figure 18b**). The reduction in antenna size after CSRR as DGS is shown in **Table 1**.

2.3.3. Use of metamaterials to enhance the antenna frequency bandwidth

In addition to the benefits of using metamaterials to design the antennas mentioned above, it is also used to enhance the antenna frequency bandwidth. To achieve this goal, the metamaterials are used as components of the antenna (**Figure 19**) or a superstrate placed above the radiation surface (like the method of improving the antenna gain), it is shown in **Figure 16b**. Unit cells of metamaterials can be placed on top or under bottom of the superstrate. The bandwidth of this antenna depends on the number of unit cells as well as the distance of the superstrate to the radiation surface.

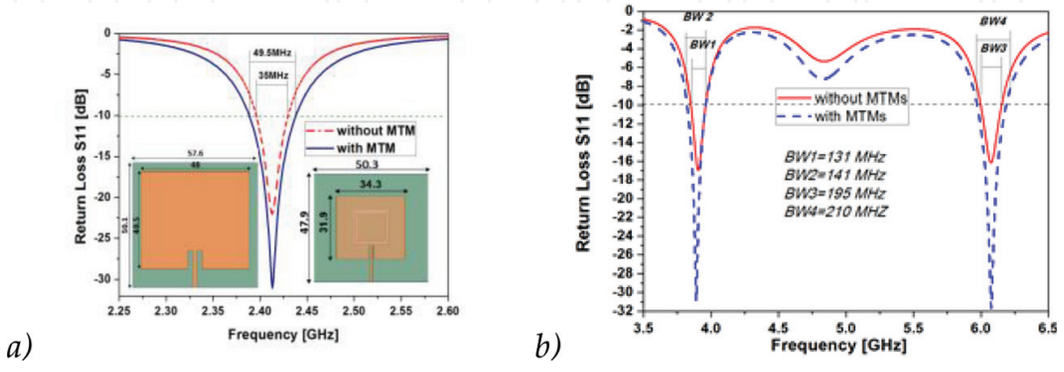

Figure 19. S-parameters of antennas without and with MTMs: as CSRR loading (a), superstrate layer for microwave C-band frequency (b) [27].

Antenna types	Antenna size ratio, %	Ratio of BW, %	Type of radiation pattern
Without MTM	100	100	Directional
With MTMs	78.7	141	Directional

Table 2. Comparison between parameters of two types of antennas for WLAN system.

Depending on the specific cases, the application of MTMs as the DGS of the antenna not only reduces the size but also increases the obtained bandwidth of the antenna. **Figure 19** compares the sizes and bandwidths of two antennas before and after applying the MTMs with the same 2.413 GHz resonant frequency for WLAN system. The ratio of the decreased size and the increased bandwidth is shown in **Table 2**.

The application of metamaterials in antenna design has enhanced its bandwidth. Depending on the technical requirements of the designed antenna, the different metamaterial structures and different application methods are selected to achieve the most appropriate antenna bandwidth.

2.3.4. Use metamaterials to get multiband

From the need to integrate multiple functions (many communication systems operation) on single devices, multiband antennas are more interested. The use of metamaterials in antenna design is an attractive trend not only to reduce size, improve the power gain, enhance bandwidth, but also to design multifrequency-band antennas [46]. The unit cells of metamaterials can be used as radiation components, a part or loaded part of the ground plane of antenna. Because, MTMs can support negative refraction indexes at resonant frequencies and unit cell structures of symmetric pairs. This can be used to design multifrequency antennas with smaller dimensions than traditional one [46]. Metamaterial can be combined with a conventional or fractal microstrip antenna to create multiband antenna, in which the antenna size is determined by the lowest

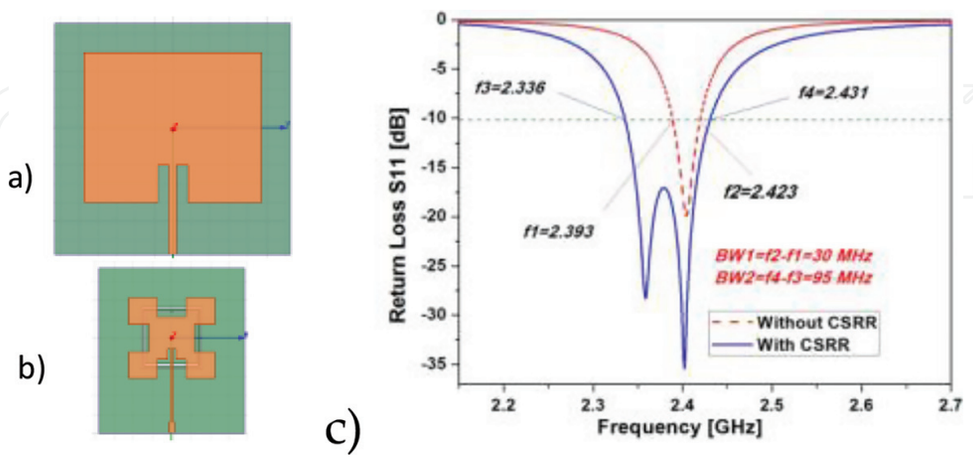

Figure 20. The configuration of microstrip antenna for WLAN systems without loaded CSRR (a), fractal antenna with loaded CSRR (b), and S_{11} parameters of them (c) [27, 48, 49].

frequency. **Figure 20** shows the simulation model and S_{11} scattering matrix coefficient of the two antennas, which operate on multiple frequencies. The resonant frequency of the antenna can be adjusted by changing the size of the antenna or the unit cell [47].

3. Conclusions

In this chapter, the applications of metamaterials in design to enhance antenna parameters are presented. The metamaterials can be applied as an environment of the antenna or as part of the antenna. Depending on the parameters of the desired antenna to improve, the metamaterials can be applied in different methods. The metamaterials can be applied to improve bandwidth, power gain, or to create compact, multifrequency-band antennas. To apply metamaterials in an antenna, the first is to design their unit cells, which are considered as atoms, creating special properties of the metamaterial at the desired frequency. The size of the unit cells is calculated, simulated, and optimized, based on the HFSS software. Effectiveness of improving the parameters of the antenna depends on the structure, size, quantity, and method of use of the unit cell of the metamaterials. Application of metamaterials in antenna design can increase their power gain ≥2 dB, bandwidth ≥100%, reduce size ≥50% or to create additional frequency bands for multicommunication systems operated antennas.

Author details

Wojciech Jan Krzysztofik[1]* and Thanh Nghia Cao[1,2]

*Address all correspondence to: wojciech.krzysztofik@pwr.edu.pl

1 Faculty of Electronics, Wroclaw University of Science and Technology, Wroclaw, Poland

2 School of Engineering and Technology, Vinh University, Nghe An, Vietnam

References

[1] Grimberg R. Electromagnetic metamaterials. Materials Science and Engineering B. 2013; **178**:1285-1295. DOI: 10.1016/j.mseb.2013.03.022

[2] Walser RM. Electromagnetic metamaterials. In Proc: SPIE 4467 Complex Mediums II: Beyond Linear Isotropic Dielectrics, San Diego, CA, USA; 2001. pp. 1-15

[3] Caloz C, Itoh T. Application of the transmission line theory of left-handed (LH) materials to the realization of a microstrip LH line. In: Proceedings of the IEEE Antennas and Propagation Society International Symposium. 2002. pp. 412-415. DOI: 10.1109/APS.2002.1016111

[4] Zheludev NI, Kivshar YS. From metamaterials to metadevices. Nature Materials. 2012;**11**: 917-924. DOI: 10.1038/nmat3431

[5] Marques R, Martin F, Sorolla M. Metamaterials with negative parameters: Theory, design and microwave applications. In: Wiley Series in Microwave and Optical Engineering. Wiley-Blackwell; 2008. ISBN: 978-0-471-74582-2. DOI: 10.1002/9780470191736

[6] Pendry JB, Holden AJ, Stewart WJ, Youngs I. Extremely low frequency plasmons in metallic meso-structures. Physical Review Letters. 1996;**76**:4773-4776. DOI: 10.1103/PhysRevLett.76.4773

[7] Pendry JB, Holden AJ, Robbins DJ, Stewart WJ. Low frequency plasmons in thin wire structures. Journal of Physics: Condensed Matter. 1998;**10**:4785-4809

[8] Sievenpiper DF, Sickmiller ME, Yablonovitch E. 3D wire mesh photonic crystals. Physical Review Letters. 1996;**76**:2480-2483. DOI: 10.1103/PhysRevLett.76.2480

[9] Sievenpiper DF, Yablonovitch E, Winn JN, Fan S, Villeneuve PR, Joannopoulos JD. 3D metallo-dielectric photonic crystals with strong capacitive coupling between metallic islands. Physical Review Letters. 1998;**80**:2829-2832. DOI: 10.1103/PhysRevLett.80.2829

[10] Ziolkowski RW, Engheta N, editors. Metamaterials Physics and Engineering Explorations. IEEE Press, A John Wiley & Sons, Inc., Publication; 2006. ISBN: 13 978-0-471-76102-0. ISBN-10 0-471-76102-8. DOI: 10.1002/0471784192

[11] Rotman W. Plasma simulation by artificial dielectrics and parallel-plate media. IEEE Transactions on Antennas and Propagation. 1962;**10**(1):82-95. DOI: 10.1109/TAP.1962.1137809

[12] Smith DR, Pendry JB, Wiltshire MCK. Metamaterials and negative refractive index. Science. 2004;**305**(5685):788-792. DOI: 10.1126/science.1096796

[13] Tretyakov S. Analytical Modeling in Applied Electromagnetics. Norwood, MA: Artech House; 2003

[14] Gangwar KP, Gangwar RPS. Metamaterials: Characteristics, process and applications. Advance in Electronic and Electric Engineering. 2014;**4**(1):97-106. ISSN 2231-1297

[15] Pendry JB, Holden A, Robbins JD, Stewart JW. Magnetism from conductors and enhanced nonlinear phenomena. IEEE Transactions on Microwave Theory and Techniques. Nov. 1999; **47**(11):2075-2084. DOI: 10.1109/22.798002

[16] Shelby RA, Smith DR, Nemat-Nasser SC, Schultz S. Microwave transmission through a two-dimensional, isotropic, left-handed metamaterial. Applied Physics Letters. 2001;**78**(4):489-491. DOI: 10.1063/1.1343489

[17] Vallecchi A, Capolino F, Schuchinsky AG. 2-D isotropic effective negative refractive index metamaterial in planar technology. IEEE Microwave and Wireless Components Letters. 2009;**19**(5):269-271. DOI: 10.1109/LMWC.2009.2017585

[18] Oliveri G, Werner DH, Massa A. Reconfigurable electromagnetics through metamaterials—A review. Proceedings of the IEEE. 2015;**103**:1034-1056. DOI: 10.1109/JPROC.2015.2394292

[19] Krzysztofik WJ, Antenna properties improvement by means of modern technology—Metamaterials as a modified substrate and/or superstrate. In: 20th M&RW, MIKON 2014, 20th International Conference on Microwave, Radar and Wireless Communications. Vol. 2. Gdansk, Poland: MIKON; 2014. pp. 637-640. ISBN 978-83-931525-2-0

[20] Krzysztofik WJ. Fractal geometry in electromagnetics applications—From antenna to metamaterials. Microwave Review. 2013;**19**(2):3-14. ISSN: 14505835

[21] Alici KB, Özbay E. Radiation properties of a split ring resonator and monopole composite. Physica Status Solidi B: Basic Research. 2007;**244**:1192-1196. DOI: 10.1002/pssb.200674505

[22] Slyusar VI. Metamaterials on antenna solutions. In: 7th International Conference on Antenna Theory and Techniques, ICATT'09; Lviv, Ukraine. 2009. pp. 19-24. DOI: 10.1109/ICATT.2009.4435103

[23] Siddiqui OF, Mo M, Eleftheriades GV. Periodically loaded transmission line with effective negative refractive index and negative group velocity. IEEE Transactions on Antennas and Propagation. 2003;**51**:2619-2625. DOI: 10.1109/TAP.2003.817556

[24] Yayun D, Wenwen L, Xijun Y, Chen Y, Houjun T. Design of unit cell for metamaterials applied in a wireless power transfer system. In: IEEE PELS Workshop on Emerging Technologies: Wireless Power Transfer. 2017. pp. 143-147. DOI: 10.1109/WoW.2017.7959382

[25] Phan DT, Phan HL, Nguyen TQH. A miniaturization of microstrip antenna using negative permittivity metamaterial based on CSRR loaded ground for WLAN applications. Journal of Science and Technology. 2016;**54**(6):689-697. DOI: 10.15625/0866-708X/54/6/8375

[26] Krzysztofik WJ. Fractals in antennas and metamaterials applications. INTECH open science, open minds. In: Brambila F, editor. Fractal Analysis–Applications in Physics, Engineering and Technology. Rijeka, Croatia: InTech; 2017. pp. 45-81. DOI: 10.5772/intechopen.68188. Print ISBN 978-953-51-3191-5, Online ISBN 978-953-51-3192-2

[27] Cao TN, Krzysztofik WJ. Metamaterials in Application for Improving the Parameters of Antennas, Telecommunication Review and Telecommunication News. Warsaw, Poland: SIGMA-NOT. pp. 300-303. DOI: 10.15199/59.2018.6.34. Yearbook XCI/LXXXVII, Notebook No. 6/2018, ISSN 1230-3496, e-ISDN 2449-7487

[28] Numan AB, Sharawi MS. Extraction of material parameters for metamaterials using a full-wave simulator. IEEE Antennas and Propagation Magazine. 2013;**55**(5):202-211. DOI: 10.1109/MAP.2013.6735515

[29] Guha D, Biswas M, Antar YMM. Microstrip patch antenna with defected ground structure for cross polarization suppression. IEEE Antennas and Wireless Propagation Letters. 2005; **4**:455-459. DOI: 10.1109/LAWP.2005.860211

[30] Singh PK, Hopwood J, Sonkusale S. Metamaterials for remote generation of spatially controllable two-dimensional array of microplasma. Scientific Reports; 2014;**4**:1-5. DOI: 10.1038/srep05964. Article number: 5964, ISSN 2045-2322

[31] Yeo J, Kim D. Design of a wideband artificial magnetic conductor (AMC) ground plane for low-profile antennas. Journal of Electromagnetic Waves and Applications. 2008;**22**:2125-2134. DOI: 10.1163/156939308787522546

[32] Cardama A, Jofre L, Rius JM, Romeu J, Blanch S, Ferrando M. "Antennas", Edicions UPC. 2nd ed. Barcelona; 2002 El Tinter, SAL (empresa certificada ISO 14001 i EMAS) La Plana 8, 08032 Barcelona ISBN: 84-8301-625-7

[33] Dewan R, Rahim MKA. Antenna performance enhancement with artificial magnetic conductor (AMC). In: 2015 IEEE Conference on Antenna Measurements & Applications (CAMA). 2015. DOI: 10.1109/CAMA.2015.7428141. ISBN: 978-1-4673-9149-8

[34] Sievenpiper DF, Zhang L, Broas RFJ, Alexopolous NG, Yablonovitch E. High-impedance electromagnetic surfaces with a forbidden frequency band. IEEE Transactions on Microwave Theory and Techniques. 1999;**47**(11):2059-2074. DOI: 10.1109/22.798001

[35] Gonzalez PJF. Multifunctional metamaterial designs for antenna applications [thesis]. Barcelon: Universitat Politecnica de Catalunya; 2015

[36] Karkkainen M, Ikonen PMT. Patch antennas with stacked split-ring resonators as an artificial magneto-dielectric substrate. Microwave and Optical Technology Letters. 2005; **46**(6):554-556. DOI: 10.1002/mop.21048

[37] Ikonen PMT, Rozanov KN, Osipov AV, lo PA, Tretyakov SA. Magneto-dielectric substrates in antenna miniaturization: Potential and limitations. IEEE Transactions on Antennas and Propagation. 2006;**54**(11):3391-3399. DOI: 10.1109/TAP.2006.884303

[38] Cao WP, Shafai L, Wang BZ, Li SM, Li BB. A small and bandwidth-extended dipole antenna with non-periodic left-handed transmission line loading. IEEE Antennas and Wireless Propagation Letters. 2014;**13**:1019-1022. DOI: 10.1109/LAWP.2014.2326433

[39] Caloz C, Sanada A, Itoh T. A novel composite right−left handed coupled-line directional coupler with arbitrary coupling level and broad bandwidth. IEEE Transactions on Microwave Theory and Techniques. 2004;**52**(3):980-992. DOI: 10.1109/TMTT.2004.823579

[40] Gao XJ, Oguz O. Enhancement of gain and directivity for microstrip antenna using negative permeability metamaterial. International Journal of Mathematics and Computer Science. 2016;**45**:880-885. DOI: 10.1016/j.aeue.2016.03.019. ISSN: 2305-7661

[41] Kim D, Choi J. Analysis of antenna gain enhancement with a new planar metamaterial superstrate: An effective medium and a fabry-pérot resonance approach. Journal of Infrared, Millimeter, and Terahertz Waves. 2010;**31**(11):1289-1303. DOI: 10.1007/s10762-010-9712-2

[42] Mosallaei H, Sarabandi K. Design and modelling of patch antenna printed on magneto-dielectric embedded-circuit meta-substrate. IEEE Transactions on Antennas and Propagation. Jan. 2007;**55**(1):45-52. DOI: 10.1109/TAP.2006.886566

[43] Liu Y, Guo X, Gu S, Zhao X. Zero index metamaterial for designing high-gain patch antenna. International Journal of Antennas and Propagation. 2013. pp. 1-12. DOI: 10.1155/2013/215681. Article ID 215681

[44] Cao TN, Krzysztofik WJ. Multiband fractal antenna for C-band ground station of satellite TV in ITU region-3. In: 21th MIKON, 6th MRW International Microwave and Radar Conference. 9–11 May 2016, Krakow, Poland; 2016. ISBN: 978-1-5090-2214-4/16/$31.00 ©2016 IEEE

[45] Raval F, Kosta YP, Joshi H. Reduced size patch antenna using complementary split ring resonator as defected ground plane. International Journal of Electronics and Communications. 2015;**69**:126-1133. DOI: 10.1016/j.aeue.2015.04.013

[46] Rajkumar R, Kiran KU. A compact metamaterial multiband antenna for WLAN/WiMAX/ITU band applications. International Journal of Electronics and Communications. May 2016;**70**(5):599-604. DOI: 0.1016/j.aeue.2016.01.025. ISSN 1434-8411

[47] Dakhli S, Rmili H, Floch JM, Sheikh M, Dobaie A, Mahdjoubi K, Choubani F. Ziolkowski RW. Printed multiband metamaterial inspired antennas. Microwave and Optical Technology Letters. June 2016;**58**(6):1281-1289. DOI: 10.1002/mop.29792

[48] Yu K, Li Y, Wang Y. Multi-band metamaterial-based microstrip antenna for WLAN and WiMAX applications. In: 2017 International Applied Computational Electromagnetics Society Symposium–Italy (ACES). 2017. pp. 6-30. DOI: 10.23919/ROPACES.2017.7916032

[49] Krzysztofik WJ, Cao TN. Fractal antenna of MIMO system WLAN. In: 12th European Conference on Antennas and Propagation (EuCAP 2018). London, UK: ExCel; 2018. pp. 1-5. ISBN: 978-1-78561-815-4, e-ISBN: 978-1-78561-816-1, ISSN 0537-9989

IntechOpen